Direct measurement of the temporal profile of the amplification gain of the transient collisional excitation neonlike manganese x-ray laser medium

N. Hasegawa, T. Kawachi, A. Sasaki, M. Kishimoto, K. Sukegawa, M. Tanaka, R. Z. Tai,* Y. Ochi, M. Nishikino, K. Nagashima, and Y. Kato

Quantum Beam Science Directorate, Japan Atomic Energy Research Agency, 8-1 Umemidai, Kizu, Kyoto, 619-0215 Japan

(Received 15 December 2006; published 8 October 2007)

The temporal profile of the amplification gain of the neonlike manganese x-ray laser in the transient collisional excitation scheme was measured by the use of the 29th-order harmonic light at a wavelength of 26.9 nm as a probe beam. The raise-up time of the gain was delayed by 20 ps from the peak of the pumping laser pulse, and the duration of the gain was 50 ps. This method is a promising powerful tool to realize the highly coherent x-ray laser beam by using a combination of an x-ray seeder and an x-ray amplifier.

DOI: 10.1103/PhysRevA.76.043805 PACS number(s): 42.55.Vc, 42.62.Fi, 52.70.−m, 78.47.+p

The recent progress in high irradiance lasers makes it possible for us to realize compact, high-repetition soft-x-ray lasers (XRL) in the transient collisional excitation (TCE) scheme [1–4]. In order to use TCE x-ray lasers in applicable research fields such as material science [5,6] and soft-x-ray imaging [7], further improvement of the performance of the TCE laser is necessary. Therefore as good an understanding as possible is required of the mechanism of generation of population inversion in plasmas. For an example the peak gain coefficient, which is commonly determined experimentally, can be reproduced by use of sophisticated theoretical model calculations [8,9], however, the temporal behavior of the gain, e.g., the duration and the raise-up time, is not understood clearly so far. Although several experiments have been conducted to measure the duration of the XRL pulse, only a few experiments have the objective to determine the temporal behavior of the population inversion density [10–12]. Since one of the most urgent subjects in XRL research is generation of a highly coherent x-ray laser beam by using a combination of an x-ray seeder and an x-ray amplifier [13,14], characterization of temporal behavior of the x-ray amplifier is indispensable for the synchronization of the seed x ray and x-ray amplifier.

Quite recently a French group measured the temporal behavior of the gain of the palladiumlike xenon XRL in the optical field ionization (OFI) scheme by injecting high-order harmonic light as a probe beam [15], and it was found that the gain was raised up within a few ps after the pumping laser pulse. In the OFI scheme, the ions are ionized up to XRL medium ions instantaneously by the laser electric field, and the population inversion is generated with a short delay corresponding to the electron impact excitation rate (this is in accordance with the result in Ref. [15]). However, in the case of XRL using a solid target pumped by linearly focused laser light, e.g., a conventional normal incidence scheme or a grazing incidence pumping (GRIP) scheme [16–18], the XRL medium ions are produced from a lower ionization stage in the preformed plasma by inverse bremsstrahlung heating, therefore the raise-up time of the population inversion strongly depends upon the ionization time up to the appropriate (neonlike, etc.) ionization stage.

In this paper, the neonlike manganese ion laser is taken as an example, and we measure the temporal behavior of the gain of the TCE laser with the solid target.

The experimental setup is shown in Fig. 1. In the first part, a Ti:sapphire laser with 20 mm diameter and 2.5 mJ energy was focused by a concave lens with a focal length of 2000 mm in an Ar gas jet target with a gas pressure of 30 torr. The spectral profile of the fundamental laser was Gaussian with 13 nm width [full width at half maximum (FWHM)] and a duration of 80 fs. The diameter of the focal spot was 100 μm, which corresponded to the peak intensity of 2×10^{14} W/cm^2. The central wavelength of the fundamental light was varied in this experiment. The details of the determination of the wavelength are described later.

In the second part, the neonlike manganese XRL medium was generated from a manganese slab target irradiated by a line-focused JAEA 20 TW CPA Nd:glass laser [3]. The width and the length of the line focus were 200 μm and 5 mm, respectively. The axis of the plasma column was aligned to that of the harmonic light. The distance between the plasma column and the gas jet target was 50 mm. The Nd:glass laser light consisted of three pulses, the first prepulse, the second prepulse, and the main pulse. The first prepulse generated the preformed plasma to increase the absorption efficiency of the following pulses. The second prepulse controlled the size and the density gradient of the plasma. The main pulse heated the plasma to ionize the ions up to the neonlike ion and produced the population inversion between $2p^53s$ and

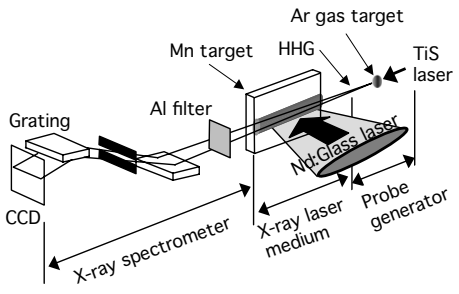

FIG. 1. Experimental setup.

*Also at Shanghai Synchrotron Radiation Facility Shanghai Institute of Applied Physics Chinese Academy of Sciences, 800-204, Shanghai 201800, China.

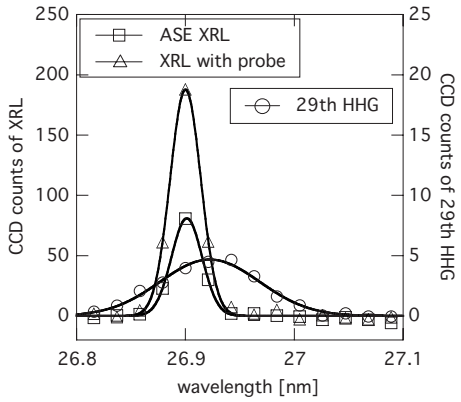

FIG. 2. The spectrum of the 29th-order harmonic line (open circles) and the neonlike manganese XRL lines measured by the x-ray spectrometer. Open squares and open triangles show the ASE XRL and the XRL with probe beam, respectively. The spectrum width of the XRL was determined by the instrumental width of the x-ray spectrometer (~0.04 nm). The spectral bandwidth of XRL line was covered by that of the 29th-order harmonic line.

$2p^5 3p$ excited levels. The energy ratio of these pulses was 2:1:8, each duration was 10, 400, and 10 ps, respectively. The pulse separation between the first prepulse and the second prepulse was 850 ps and that between the second prepulse and the main pulse was 250 ps, respectively. The total irradiation energy was 9 J. The intensities of these pulses were 1.6×10^{13}, 2.0×10^{11}, and 6.3×10^{13} W/cm^2, respectively.

The oscillator of the Ti:sapphire laser and that of the CPA Nd:glass laser were synchronized with the phase synchronizer (Spectra-Physics "Lock-to-clock"). Timing jitter at the manganese target position between both the lasers was measured to be better than ±3 ps by use of the streak camera (HAMAMATU FESCA200), which is smaller than the predicted lifetime of the population inversion of the XRL.

In the third part, the generated x-ray beam was observed by the grazing incidence spectrometer set on the axis of the harmonic light. In order to cut the fundamental Ti:sapphire laser light, the 0.8 μm thick aluminum filter was put in front of the spectrometer. The x-ray beam was collected by the grazing incidence Au/Cr coated spherical mirror with a curvature of 3120 mm, went through the 100 μm wide entrance slit, was dispersed by the SHIMADZU flat field holographic grating with 1200 grooves/mm, and was vertically focused (the direction of wavelength dispersion) on the focal plane. The back-illuminated charged coupled device (CCD, Princeton SXTE-1024) was used as the x-ray detector. The instrumental width of this spectrometer was 0.04 nm at the wavelength of the neonlike manganese x-ray laser (=26.9 nm) and it was enough to measure the spectral width of the harmonic light.

In order to obtain the spectral matching between the neonlike manganese XRL and the harmonic light, we adjusted the central wavelength of the Ti:sapphire laser with monitoring the XRL line and the 29th-order harmonic line by the x-ray spectrometer. Figure 2 shows the spectrum of the 29th-order harmonic line for the central wavelength of the Ti:sapphire laser of 780.1 nm (open circles) together with the amplified spontaneous emission (ASE) of the XRL line (open squares). Both the data were fitted by Gaussian curves (see solid curves). The spectral width, the output energy, and the horizontal beam divergence of the 29th-order harmonic line were 0.12 nm, 0.1 nJ (±0.02 nJ), and 1.4 mrad (±0.2 mrad), respectively. The source size of the 29th-order harmonic light (=r), estimated from the beam divergence (=θ) and the wavelength (=λ), was expected to be $r=1.22\lambda/\theta=23$ μm (±3 μm) which was smaller than the focal spot size of the fundamental laser light. The beam profile of the 29th-order harmonic light at the edge of the XRL medium could be treated as the far-field image, because the condition of the Fraunhofer diffraction ($d>2r^2/\lambda$) was satisfied with the distance from the source point to the XRL medium ($d=50$ mm). Therefore the diameter of the 29th-order harmonic light at the edge of the XRL medium was estimated to be 70 μm (±10 μm). It should be noted that the obtained linewidth of the XRL line was determined by the instrumental width of the x-ray spectrometer (~0.04 nm), although the actual width of the XRL line was expected to be much smaller (~0.006 nm). In Fig. 2, the open triangles show the spectrum of the XRL line under the condition that the probe beam (29th-order harmonic light) is injected into the XRL medium at 32 ps delay time measured from the peak of the main pulse of the Nd:glass laser. The output energy of the XRL with the probe beam injection was increased compared with that of the ASE XRL. The net increase of the output energy or the energy of the amplified probe beam, E_{XRL}, was measured to be 2.2 nJ.

Here we estimate the small signal gain, $\mathcal{G}$, of the XRL medium: $\mathcal{G}$ can be described with the input energy of the probe beam (E_{probe}), E_{XRL}, and the coupling efficiency between the XRL and the 29th-order harmonic light in spectrum (ε_ν) and in space (ε_s), i.e., $\mathcal{G}=E_{XRL}/\varepsilon_\nu\,\varepsilon_s\,E_{probe}$. ε_ν is the ratio of the spectral width of XRL ($\Delta\lambda_{XRL}$) to that of the probe beam ($\Delta\lambda_{probe}=0.12$ nm), $\Delta\lambda_{XRL}/\Delta\lambda_{probe}$, and it is 0.047, where $\Delta\lambda_{XRL}$ is estimated to be 0.0056 nm from the result of measurement of neonlike selenium XRL [19]. ε_s is described from overlap of the XRL medium and the probe beam. The cross section of the XRL medium is a rectangle of 200 μm (focal width of the Nd:glass laser) in 40 μm (±10 μm) (see the hydrodynamic simulation in Fig. 5 and Ref. [20]), and the diameter of the probe beam is 70 μm. Therefore ε_s is estimated to be 0.68 (±0.19). Under the condition of $E_{probe}=0.1$ nJ, and $E_{XRL}=2.2$ nJ, we obtain $\mathcal{G}=690(\pm240)$.

Figure 3 shows the horizontal beam profile of the XRL under the condition that the probe beam is injected into the XRL medium at various delay times measured from the peak of the main pulse of the Nd:glass laser. The direction of the probe beam was set to parallel to the target surface. The beam divergence of the amplified spontaneous emission (ASE) of XRL was 5 mrad. From 32–42 ps delay time, the beam divergence became narrower than that of the ASE XRL, and the angles of the peak were obtained in almost the same position to that of the probe beam. This implied that the probe beam went through the whole plasma column (=5 mm). The details of the electron density and the electron density gradient are described later.

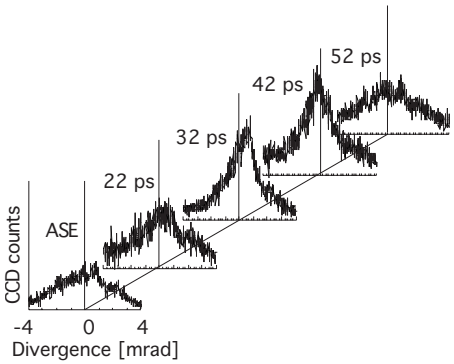

FIG. 3. The horizontal beam profiles of the XRL under the condition that the probe beam was injected at various delay times. The beam divergence was obviously improved compared with the ASE XRL at the 32 and 42 ps delay time.

In Fig. 3, in order to obtain the temporal behavior of the gain, we subtracted the ASE component from the obtained XRL profile as follows: We assumed that the side portion of each spectrum ($>\pm 1.5$ mrad) was dominated by the ASE component, and the profile of the ASE signal was multiplied by a factor to adjust to the side portion of each spectrum. The net amplified component was obtained by subtracting the ASE spectrum from each spectrum. Figure 4 shows the temporal behavior of the small signal gain ($\mathcal{G}$) of the neonlike manganese XRL medium (open circles). The dashed curve is the temporal profile of the main pulse of the Nd:glass laser. The abscissa is the delay time measured from the peak of the main pulse. The uncertainty in time was from the timing jitter between the Ti:sapphire laser and the Nd:glass laser (± 3 ps). The error bar of the $\mathcal{G}$ was determined by the uncertainty of the spatial coupling efficiency (ε_s) and that of the energy of the probe beam (E_{probe}). From this result the raise-up time of the $\mathcal{G}$ was clearly separated from the main laser pulse. The peak value of the $\mathcal{G}$ (~ 810) was obtained at 37 ps delay time. It corresponded to the gain length product and gain coefficient of $gl=6.7$ and $g=13.4$ cm^{-1}, respectively. The raise-up time of the gain was measured to be

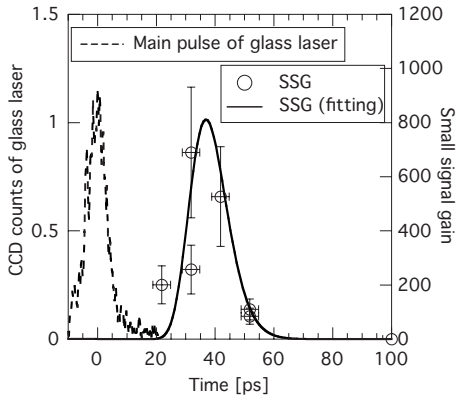

FIG. 4. The temporal behavior of the small signal gain ($\mathcal{G}$) of the neonlike manganese XRL medium (open circles) and the temporal profile of the main pulse of the Nd:glass laser (dashed curve). The peak of the $\mathcal{G}$ was 810 at 37 ps delay time.

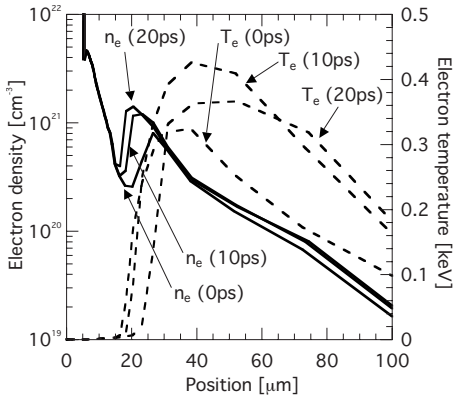

FIG. 5. The spatial profile of the electron density (n_e, solid curves) and the electron temperature (T_e, dashed curves) calculated by HYADES code. The peak of T_e (~ 400 eV) was obtained at around $n_e=1.5\times 10^{20}$ cm^{-3}. The size of the XRL gain region in the direction of plasma expansion was about 40 μm.

20 ps, the details of the temporal behavior of the gain are described later.

We calculated the temporal behavior of the population inversion density for the present experimental condition and compared the present experimental result with the calculation. The plasma parameters [electron temperature T_e, electron density n_e, and electron density gradient grad(n_e)] were calculated by 1D Hydrodynamic code HYADES [21]. The population inversion density was calculated by using an atomic kinetics code based on HULLAC code [22] which treated $n=3$ excited levels with the fine structure resolved, $n=4$, 5, 6, excited levels with angular momentum resolved and $n=7$, 8 with hydrogenic approximation. Figure 5 shows the calculated spatial profile of the electron density n_e (solid curves) and electron temperature T_e (dashed curves) at $t=0$, 10, and 20 ps under the experimental pumping condition, where t is measured from the peak of the main pulse. The abscissa is the position from the target surface. At $t=20$ ps, in which the gain was generated in the present experiment, the calculated result indicated that the peak of T_e ($=350-400$ eV) was obtained at around $n_e=0.8-4.0\times 10^{20}$ cm^{-3} and grad(n_e) $\sim 5.0\times 10^{22}$ cm^{-4} at the position of $30-70$ μm from the target surface. The propagation length of the XRL in the plasma column estimated from the electron density gradient was $[2n_c d/\mathrm{grad}(n_e)]^{1/2}=5.0$ mm, where n_c was the critical density of the wavelength of 26.9 nm ($=1.5\times 10^{24}$ cm^{-3}) and d was the size of the gain region in the direction of plasma expansion (~ 40 μm). In the case where the main pulse energy was deposited in the higher n_e region ($=4-8\times 10^{20}$ cm^{-3}), Fig. 5 shows that the density gradient was large [grad(n_e) $\sim 5\times 10^{23}$ cm^{-4}]. The propagation length of the ASE XRL and the probe beam was too short to realize substantial lasing ($[2n_c d/\mathrm{grad}(n_e)]^{1/2}$ ~ 1.6 mm). Therefore substantial lasing was obtained in the low n_e region ($=0.8-4.0\times 10^{20}$ cm^{-3}).

Since the collisional excitation rate and the collisional-radiative ionization rate were quite sensitive to n_e and rather insensitive to T_e [23], we fixed $T_e=400$ eV and calculated the temporal behavior of the population inversion density for

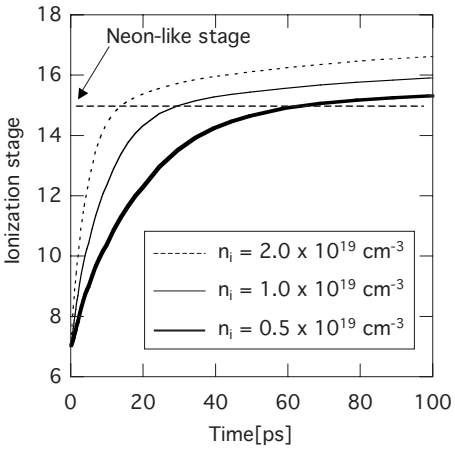

FIG. 6. The temporal behavior of the averaged ionization stage of manganese ions for various n_i under the condition that T_e =400 eV. The dashed line indicates the neonlike ion (Z=15). Under the condition that n_i=2.0×10^{19} cm^{-3}, the ionization stage was over the neonlike ionization stage within 20 ps.

various ion density (n_i). Figure 6 shows the calculated result for the temporal behavior of the averaged ionization stage ($Z_{average}$) of manganese ions for various n_i. The dashed line shows the ionization stage of the neonlike ion (=15). The calculated result indicates that the ionization time strongly depends upon the ion density (or the electron density). Figure 7 shows the temporal profile of the gain from the present experiment (open squares) and from the calculation of the gain for various n_e (thin curves). The raise-up time and the duration of the gain were measured to be 20 and 50 ps, respectively. The spatially integrated XRL gain (bold solid curve) was obtained by integrating the calculated result of

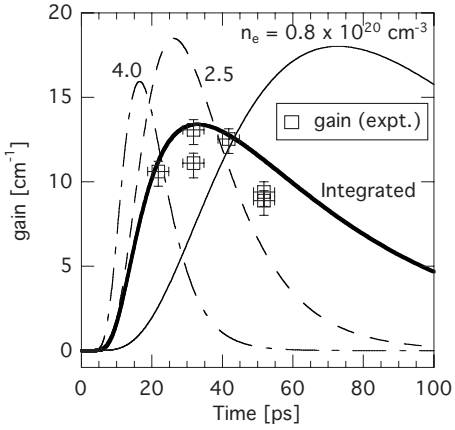

FIG. 7. The temporal behavior of the experimental gain (open squares) and the calculated gain for n_e=0.8, 2.5, and 4.0 ×10^{20} cm^{-3} (thin curves). The raise-up time and the duration of the experimental gain were 20 and 50 ps, respectively. The spatially integrated XRL gain (bold solid curve) was obtained by integrating the temporal XRL gain profiles for the electron density ranging from 0.8×10^{20}–4.0×10^{20} cm^{-3}.

the temporal XRL gain profiles for the electron density ranging from 0.8×10^{20}–4×10^{20} cm^{-3}. The peak value of the spatially integrated gain was adjusted to that of the present experiment (=13.4 cm^{-1}). The result of the calculation of the spatially integrated gain profile was in good agreement with the experiment.

It is quite valuable to compare the present result with other experimental and theoretical results. Mocek *et al.* [15] measured the raise-up time of the palladiumlike xenon laser in the OFI scheme, and the obtained raise-up time was less than 5 ps. Wang *et al.* [14] measured the raise-up time of the neonlike titanium laser in the TCE scheme with the grazing incident pumping method, and the raise-up time was 2–4 ps. Strati *et al.* [8] showed the calculated raise-up time of ~5 ps in the neonlike germanium laser in the TCE scheme using EHYBRID code [24]. The present raise-up time was much longer than these investigations.

In the case of OFI scheme [15], since the XRL medium ions are instantaneously produced by the laser electric field, the raise-up time is mainly originated from the excitation time which is less than 5 ps, whereas our theoretical calculation implies that the present raise-up time was mainly determined by the ionization time from the lower-ionization stage in the preformed plasma to the neonlike ion (see Fig. 6).

In comparison with the result by Wang *et al.* [14], the electron density expected from the incident angle of the pumping laser was 2.6×10^{20} cm^{-3}, which was comparable with that in the present experiment case, whereas the raise-up time was much shorter than our result. This discrepancy might be due to that the ionization stage in the preformed plasma in Ref. [14] was much higher than that in the present case ($Z_{average}$~7).

In comparison with the calculated result by using EHYBRID [8,24], the difference may be due to the following: Because the ionization time is virtually proportional to the reciprocal number of n_e, if the pumping laser energy is deposited in the higher density region, the ionization time (or the raise-up time of the gain) becomes shorter. Indeed, Ref. [8] suggested that the main pulse energy was deposited in the higher n_e region (~5×10^{20} cm^{-3}), which was higher than that in the present case.

The present result shows that the seed x-ray or probe beam is successfully amplified in the x-ray amplifier generated from a solid target. The beam divergence of the output x-ray laser beam was improved compared with that of the ASE signal. In addition to it, due to the narrow spectral bandwidth of the XRL medium compared with that of the harmonic light, XRL medium works as frequency filter of the harmonic light and chooses the temporally coherent component of the harmonic light resulting in having the possibility of improvement in the temporal coherence of XRL beam [25]. Improvement of the temporal coherence of XRL is an important subject, however, it is out of the focus of this paper.

In summary, we succeeded to measure the temporal behavior of the gain of the XRL medium from a solid target in

the TCE scheme by injecting the probe beam into the XRL medium. It was found that the raise-up time of the gain was sensitive to the ionization stage in the preformed plasma and was longer than that in other experiments. The present result indicates that the method of injecting the probe beam into the XRL medium is a powerful tool to realize a highly coherent x-ray laser beam by using the combination of an x-ray seeder and an x-ray amplifier.

[1] M. P. Kalachnikov *et al.*, Phys. Rev. A **57**, 4778 (1998).
[2] J. Filevich, K. Kanizay, M. C. Marconi, J. L. A. Chilla, and J. J. Rocca, Opt. Lett. **25**, 356 (2000).
[3] T. Kawachi *et al.*, Phys. Rev. A **66**, 033815 (2002).
[4] Ph. Zeitoun *et al.*, Nature (London) **431**, 23 (2004).
[5] R. Z. Tai *et al.*, Phys. Rev. Lett. **89**, 257602 (2002).
[6] R. Z. Tai, K. Namikawa, A. Sawada, M. Kishmoto, M. Tanaka, P. Lu, K. Nagashima, H. Maruyama, and M. Ando, Phys. Rev. Lett. **93**, 087601 (2004).
[7] M. G. Capeluto *et al.*, in *X-Ray Lasers 2004*, edited by J. Zhang, IOP Conf. Proc. No. 186 (Institute of Physics, London, 2004), p. 521.
[8] F. Strati *et al.*, Central Laser Facility Annual Report No. 52, 1999/2000.
[9] J. Nilsen and J. Dunn, Proc. SPIE **4505**, 100 (2001).
[10] Y. Ochi *et al.*, Appl. Phys. B: Lasers Opt. **78**, 961 (2004).
[11] A. Klisnick *et al.*, Phys. Rev. A **65**, 033810 (2002).
[12] F. Staub, M. Braud, J. E. Balmer, and J. Nilsen, Phys. Rev. A **72**, 043813 (2005).
[13] S. Sebban *et al.*, in *X-Ray Lasers 2006*, edited by P. V. Nickls and K. A. Janulewicz, Springer Proceedings in Physics No. 115 (Springer, Berlin, 2006), p. 225.
[14] Y. Wang, E. Granados, M. A. Larotonda, M. Berrill, B. M. Luther, D. Patel, C. S. Menoni, and J. J. Rocca, Phys. Rev. Lett. **97**, 123901 (2006).
[15] T. Mocek *et al.*, Phys. Rev. Lett. **95**, 173902 (2005).
[16] R. Keenan *et al.*, Proc. SPIE **5197**, 213 (2003).
[17] B. M. Luther, Y. Wang, M. A. Larotonda, D. Alessi, M. Berrill, M. C. Marconi, J. J. Rocca, and V. N. Shlyaptsev, Opt. Lett. **30**, 165 (2005).
[18] A. Weith, M. A. Larotonda, Y. Wang, B. M. Luther, D. Alessi, M. C. Marconi, J. J. Rocca, and J. Dunn, Opt. Lett. **31**, 1994 (2006).
[19] J. A. Koch, B. J. MacGowan, L. B. DaSilva, D. L. Matthews, J. H. Underwood, P. J. Batson, R. W. Lee, R. A. London, and S. Mrowka, Phys. Rev. A **50**, 1877 (1994).
[20] M. Tanaka *et al.*, Surf. Rev. Lett. **9**, 641 (2002).
[21] G. J. Pert, J. Fluid Mech. **131**, 401 (1983).
[22] M. Klapisch and A. Bar-Shalom, J. Quant. Spectrosc. Radiat. Transf. **58**, 687 (1997).
[23] T. Fujimoto, J. Phys. Soc. Jpn. **54**, 2905 (1985).
[24] J. T. Larsen and S. M. Lane, J. Quant. Spectrosc. Radiat. Transf. **51**, 179 (1994).
[25] N. Hasegawa *et al.*, in *X-Ray Lasers 2004*, edited by J. Zhang, IOP Conf. Proc. No. 186 (Institute of Physics, London, 2004), p. 273.